Volume 17, Issue 2, 172510 (1-6)

Iranian Journal of Earth Science (IJES)

https://doi.org/10.57647/j.ijes.2025.1702.10

Numerical analysis of fluid flow behavior in micro fracture of coal matrix

Harinandan Kumar[1,*], Nirlipta Priyadarshini Nayak[1], Rose Havilah Pulla[2], Betty Joseph[1], Amrutha Ashok[1], Devika Lal Karukayil Manilal[1]

[1] *Department of Petroleum Engineering and Earth Sciences (Energy Cluster) (SOE), University of Petroleum and Energy Studies, Bidholi, Dehradun, India.*
[2] *Department of Chemical Engineering (Energy Cluster) (SOE), University of Petroleum and Energy Studies, Bidholi, Dehradun, India.*

[*] **Corresponding author:** harinandankumar88@gmail.com

Original Research

Received:
24 April 2024
Revised:
13 August 2024
Accepted:
10 September 2024
Published online:
10 April 2025

Abstract:

Coal beds are very complex porous media that exhibit heterogeneity, dual-porosity, and stress sensitivity. Simulation models for fluid flow from coal matrix for coal bed methane (CBM) and enhanced coal bed methane (ECBM) recovery have significantly progressed in recent decades. Analytical models have limitations or challenges in application due to assumptions and oversimplification. Therefore, in this study, numerical modeling and simulations were carried out to investigate the fluid flow behavior in the microchannel of the coal matrix. A variation in pressure drop was considered to evaluate the flow pattern in the coal matrix. Analysis was carried out to assess the effect of pressure drop on fluid velocity in the microchannel. The results of the simulations indicated an increased fluid velocity with pressure drop. Well-developed and connected microchannel was significant for transporting fluid in the coal matrix. The Simulation results were found helpful in estimating the critical pressure drop to enhance fluid flow in the microchannel of the coal matrix.

Keywords: Coal matrix; Microchannel; Fluid velocity; Numerical analysis

1. Introduction

The coal matrix stores the maximum amount of methane in its porous structure. The transportation of methane within the coal matrix is only possible by the proper connectivity between the pores and fracture channel. The microfracture in the coal matrix facilitates good connectivity between pores and microchannels during gas transportation. This micro and macro channel is susceptible to reservoir parameters like pressure. A decline in pore pressure raises effective stress and causes the narrowing or closer of fractures. The reduction in fracture aperture reflects the declining methane production rate during gas transportation. Therefore, a detailed study of flow patterns with pressure drop is essential to evaluate the feasibility and recovery rate in the CBM production process.

The effect of pressure depletion on the deformation of the coal matrix and change in fracture aperture was studied elsewhere (Clarkson et al., 2010; Clarkson et al., 2013; Wei and Zhang, 2013; Kumar et al., 2017). The studies showed reduced permeability due to the narrowing and closing of the fracture aperture at lower pore pressure. An increase in adequate pressure leads to the crushing of the cleat structure. Ma et al. (2017) studied the impact of geomechanical parameters on coal beds and concluded with flow patterns during the CBM production process. A reduction in permeability with an increase in stress parameters was observed during the investigation. The decline in permeability was due to the narrowing or closure of the fracture at a higher stress value. Wang et al. (2019) studied the interaction of coal matrix with permeability at variable pressure. A reduced permeability was observed with downstream pressure. The reduction in permeability was attributed to the change in cleat structure and deformation in the coal matrix. Thus, a variation in reservoir pressure resulted in deformation in the coal matrix, change in fracture aperture, and flow pattern in the coal matrix. Investigating changes in flow patterns with pressure at a laboratory scale is costly and time-consuming. Therefore, the analytical and numerical model is used to visualize flow patterns in coal seams at variable pressure. The researchers proposed many models to correlate the flow pattern with changes in pore pressure.

Ramanandraibe et al. (2021) developed a reservoir model to study the formation's multilayer and permeability anisotropy effects. Results were concluded with higher productivity at a lower permeability anisotropy ratio. Li and Liu (2022), Dehghan and Yazdi (2023) used Monte Carlo and Box Muller methods to determine gas flow characteristics in the coal bed. The fracture in the plastic zone was found beneficial for fluid flow in the coal bed. A decline in permeability was observed with creep deformation in fracture.

Previous studies have been carried out to determine the flow behavior in microchannels while the connectivity and flow through the microchannel are essential for the continuity of flow. Therefore, numerical modeling and simulation were carried out to study the impact of reservoir parameters on fluid flow behavior in coal beds. The fluid flow in macro fractures was studied in detail and reported elsewhere (Dabiri et al., 2017; Zhang et al., 2019; Ye et al., 2020; Yan et al., 2021). Kumar et al. (2017) used COMSOL Multiphysics to model coal deformation under fluid pressure. Results were reported with swelling in the coal matrix at elevated injection pressure. Mohanty and Pal (2016) investigated the flow characteristics in coal beds using COMSOL Multiphysics. The velocity and pressure fluctuation were determined in the coal bed under reservoir conditions (Xu et al., 2021). Studies reported the impact of reservoir parameters on the microchannel of the coal matrix during CBM production (Wei and Zhang, 2010; Fan et al., 2020). The coal matrix's microchannel is a critical feature that establishes connectivity during gas transportation. Therefore, in this research work, numerical modeling and simulation were carried out to determine the effect of pressure drop on fluid flow in the microchannel of the coal matrix. The SEM image was used for modeling, and a continuous pressure drop was assumed for the simulation. Fluid velocity was determined to predict the flow pattern in the microchannel. The novelty of the research work is towards predicting flow patterns in the microchannel of the coal bed during the CBM production process. The results will be helpful for the prediction of fluid flow in microchannels and the estimation of production rate during the CBM exploitation.

2. Geometrical model

The scanning electron microscopic image of the coal sample obtained from Jharia Coalfield India was used for modeling (Fig. 1 a). The SEM image was converted into.DXF file. The CAD drawing file was imported into COMSOL Multiphysics 5.5 version software suit (Fig. 1 b).

2.1 Description of geometrical model

The fluid flow analysis in microfractures of the coal sample obtained from the study area was carried out using the Creeping Flow (Stokes Flow) model. The model was chosen to analyze the microfracture's stoke flow in grain nuances. The modeling was carried out to determine fluid movement through the pore geometry to the surface of the porous rock at variable pressure drops. The pore-scale flow analysis was conducted elsewhere using COMSOL Multiphysics to examine the flow pattern in the porous material (Sirivithayapakorn and Keller, 2003; Auset and Keller, 2004). The Scanning electron microscopic image of 850 $\times$ 900 micrometer of coal sample obtained from the study area was collected and used for the modeling purpose (Fig. 1 b). The image is first converted to.DXF file to represent the microstructure of coal matrix in drawing form and imported into the COMSOL Software suite 5.5. The imported drawing was considered a single continuum with continuous properties throughout the model. The boundary conditions for fluid transportation were applied to the coal matrix. The input and output were assigned to the upper and lower surface of the imported drawing (Fig. 2). The symmetry was given to the wall, as shown in (Fig. 3). Methane gas with

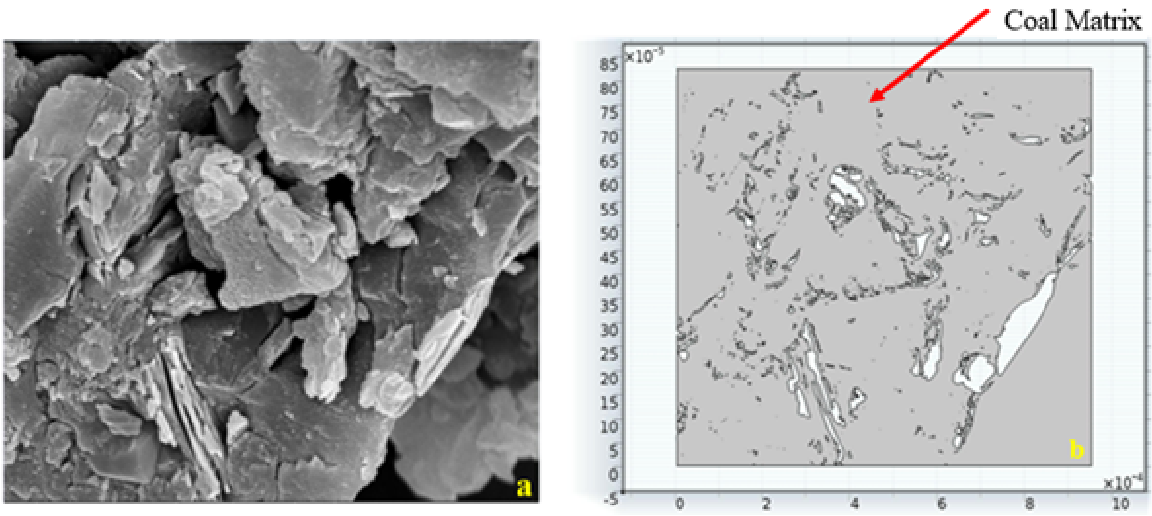

Figure 1. SEM image used for the modelling (a) SEM image of coal sample (b) SEM image converted in to .DXF format (Unit = m).

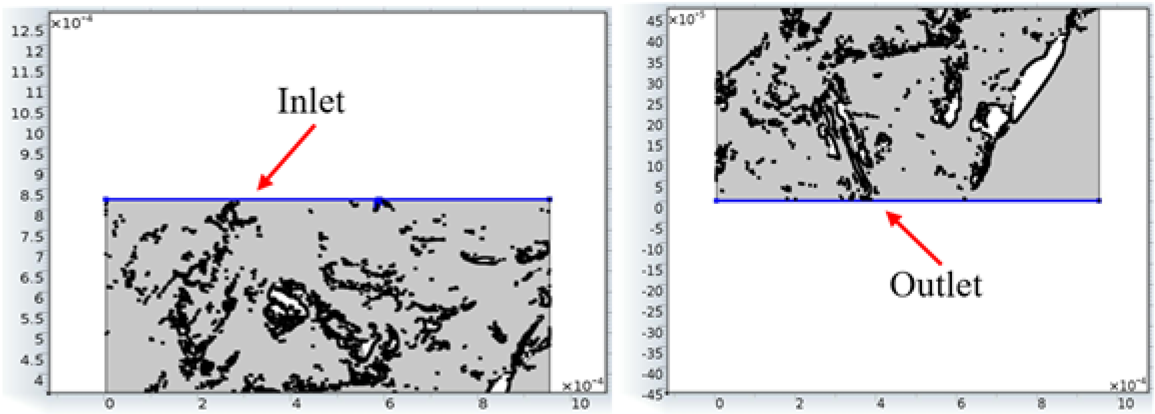

Figure 2. Assignment of Boundary condition (a) Inlet for fluid Transportation (b) Outlet for fluid Transportation.

a fluid density of 0.6038 kg/m^3 was considered to pass through the fractures. The gas was passed in such a way that it was not penetrating the solid particles. Methane was passed from inlet to outlet, and no flow zone was considered towards the symmetry.

2.2 Model definition and governing equations

The Stokes equation was considered to solve the flow of fluid in the microchannel. The equation was assumed to visualize the fluid flow pattern. Stroke equation for fluid flow in the microchannel is written as (El-Amin, 2022):

$$\mu\nabla^2 u - \nabla p = 0 \tag{1}$$

$$\nabla u = 0 \tag{2}$$

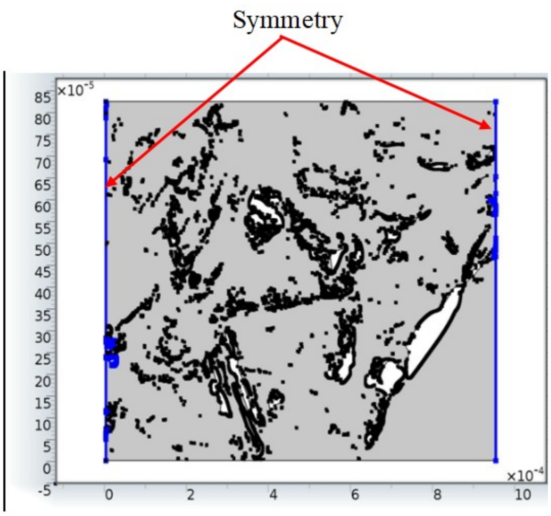

Figure 3. Assignment of symmetry into the model (dimensions are in m).

where, u = velocity of the fluid (m/s); p = pressure (Pa); μ = dynamic viscosity (Pa.s).
Force was not applied therefore it is not considered in the Equation. The explicit equation of the velocity vector is given as:

$$\mu\left(\frac{\partial^2 u}{\partial x^2}+\frac{\partial^2 u}{\partial y^2}+\frac{\partial^2 u}{\partial z^2}\right)-\frac{\partial p}{\partial x}=0 \tag{3}$$

$$\mu\left(\frac{\partial^2 v}{\partial x^2}+\frac{\partial^2 v}{\partial y^2}+\frac{\partial^2 v}{\partial z^2}\right)-\frac{\partial p}{\partial y}=0 \tag{4}$$

$$\mu\left(\frac{\partial^2 w}{\partial x^2}+\frac{\partial^2 w}{\partial y^2}+\frac{\partial^2 w}{\partial z^2}\right)-\frac{\partial p}{\partial w}=0 \tag{5}$$

$$\frac{\partial u}{\partial x}+\frac{\partial v}{\partial y}+\frac{\partial w}{\partial z}=0 \tag{6}$$

If the density is assumed constant then the Eq. 1 is modified as:

$$\nabla\mu(\nabla u+\nabla u^T)-\nabla p=0 \tag{7}$$

Brinkman equations, with the Stokes-Brinkman assumption used for the creeping flow as:

$$-\nabla p+\nabla\frac{\mu}{\varepsilon_p}(\nabla u+\nabla u^T)-\frac{\mu}{k}u=0 \tag{8}$$

where, εp is the porosity, and k is the permeability of the medium.

The porosity and permeability were calculated based on the equation as:

$$k(x,y)=\frac{k_0}{100\times im1(x,y)+0.1} \tag{9}$$

$$\varepsilon_p(x,y)=1-0.99\times im1(x,y) \tag{10}$$

Table 1. Input Data used for Simulation.

Name	Value	Unit	Description
ρ	0.6038	kg/m^3	Fluid density
μ_0	11.77×10^{-6}	Pa.s	Dynamic viscosity
Δ P	9×10^{-4} to 21×10^{-4}	Pa	Pressure drop

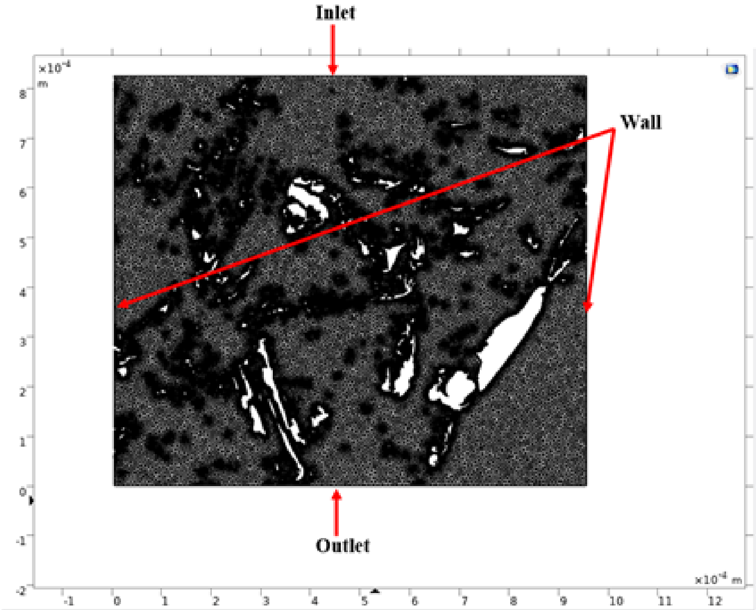

Figure 4. Meshed model for analysis.

where, *im1* = image function. The image function was derived from the imported image and varied from 0 to 1. The model was solved at a variable pressure drop. No-slip condition was considered by keeping zero velocity at the boundary. The input data used in simulation is summarized in Table 1.

3. Meshing parameters

The model was subdivided into discrete geometrical shapes using a meshing tool. The mesh cells were used for the discrete local approximation of the complete model. Discretization was performed using a free triangular element to simplify the calculation. The parameters used for the meshing are presented in Table 2. The meshed surface is shown in (Fig. 4).

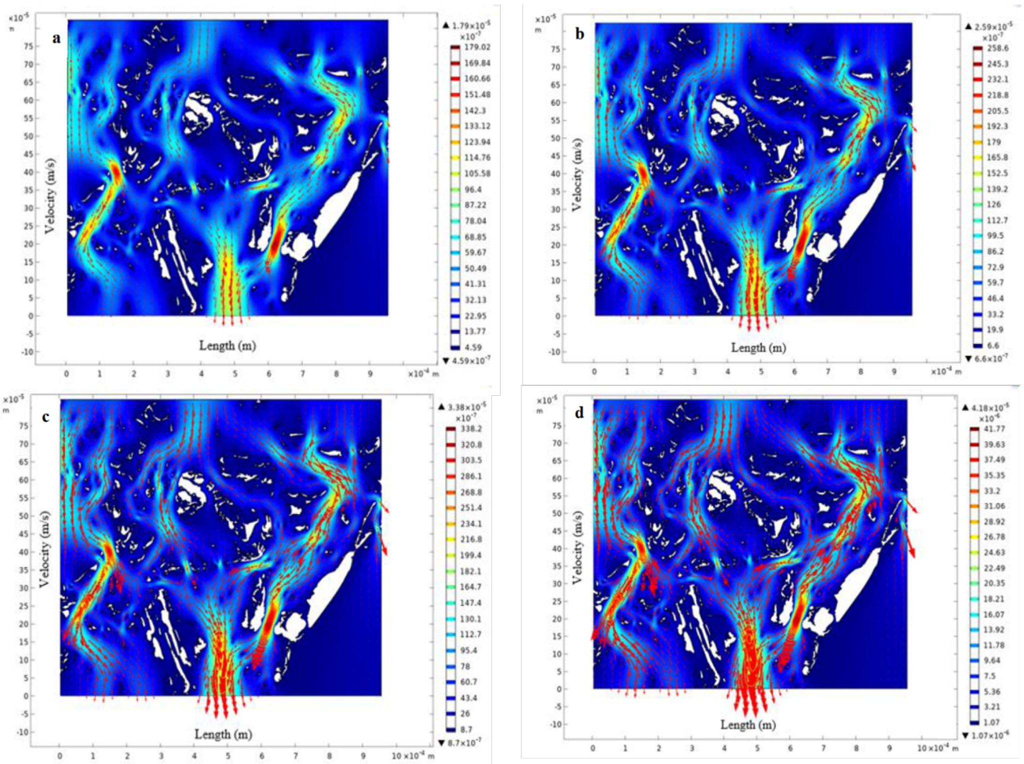

Figure 5. Velocity magnitude at variable pressure drop (a) Pressure drop at 0.000900 P'a (b) Pressure drop at 0.0001300 Pa (c) Pressure drop at 0.0001700 Pa (d) Pressure drop at 0.0002100 Pa.

Table 2. Meshing parameters for discretization of model.

Meshing parameters	Value
Mesh quality	0.9032
Elemental type (triangular)	186577
Elements (edge)	19109
Elements (edge)	13715
Sequence type	Physics-controlled
Element size	Normal

4. Results and discussion

The simulation was carried out to solve the model according to the input parameters shown in Table 1, following the Creeping Flow (Stokes Flow) model. Pressure drop varied from 9×10^{-4} to 21×10^{-4} Pa to evaluate fluid velocity in the microchannel. An increase in pressure drops, i.e., 4×10^{-4} Pa, was used in each run. The results of the velocity profile are shown in (Fig. 5). The contour profile indicated an increase in velocity with pressure drop. Fluid velocity varied from 4.59 to 179.02×10^{-7} m/s at the pressure drop 9×10^{-4} Pa (Fig. 5 a). The developed and connected microchannel was observed with smooth and continuous flow. As the pressure drop increased to 13×10^{-4} Pa, the fluid velocity raised from 6.6 to 258.6×10^{-7} m/s, indicating an extension in fracture width (Fig. 5 b). Further increment in pressure drop from 13 to 21×10^{-4} Pa surges the fluid velocity from 8.7 to 417.7×10^{-7} Pa (Fig. 5 c and 5 d). The rise in fluid velocity with pressure drop has been attributed to the extension in fracture width and higher permeability. The correlation of fluid velocity with arc length (horizontal length) shown in Fig. 6 indicated an increase in fluid velocity with pressure drop. Higher velocity was observed at pressure drop varied from 17 to 21×10^{-4} Pa. A reduction in fluid velocity between 300 to 400 μm was due to the narrow path and cross-connections. Fluid velocity was higher because the fractures were well-developed and connected with the coal matrix.

A well-developed microchannel in the coal matrix showed an increase in fluid velocity. The cross-extension area in the coal matrix hindered the gas flow. The arc length up to 150 μm indicated increased fluid velocity because of the well-developed and connected microchannel. Further connectivity of fractures was available at approx 400 to 800 μm. The fracture connectivity facilitates the continuity of flow. The connectivity of the microfracture was adequate for the continuity of flow in the coal matrix.

5. Conclusion

The results of numerical analysis for fluid flow behavior in the developed model of coal matrix are concluded as follows:

- Well-developed and connected microchannels facilitate the continuity of flow during gas transportation.
- An increase in fluid velocity was observed with an increase in pressure drop.
- An increase in velocity was attributed to the shrinkage in the coal matrix with an extension in fracture width and higher permeability.

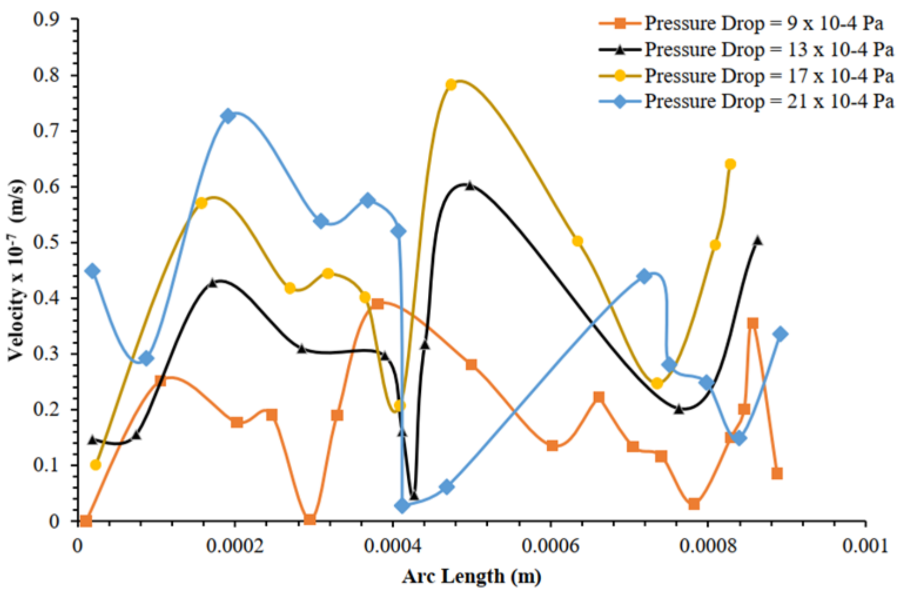

Figure 6. Correlation of fluid velocity with Arc length at variable pressure drop.

- The Cross-extension area was responsible for reducing fluid velocity in the coal matrix.
- Evaluation of critical pressure drop is essential for optimized gas transportation in the coal matrix.

Acknowledgement
This research work in terms of modeling and simulation would not have been possible without the exceptional support of our Institution University of Petroleum and Energy Studies. The software support from the institution helped us to carry out the studies.

Authors contributions
All the authors have participated sufficiently in the intellectual content, conception and design of this work or the analysis and interpretation of the data (when applicable), as well as the writing of the manuscript.

Availability of data and materials
The data that support the findings of this study are available from the corresponding author, upon reasonable request.

Conflict of interests
The authors declare that they have no known competing financial interests or personal relationships that could have appeared to influence the work reported in this paper.

References

Auset M., Keller A. A. (2004) Pore-scale processes that control dispersion of colloids in saturated porous media. *Water Resources Research* 40:503. DOI: https://doi.org/10.1029/2003WR002800.

Clarkson C. R., Pan Z., Palmer I. D., Harpalani S. (2010) Predicting sorption-induced strain and permeability increase with depletion for coalbed-methane reservoirs. *SPE Journal* 15:152–159. DOI: https://doi.org/10.2118/114778-PA.

Clarkson C. R., Qanbari F., Nobakht M., Heffner L. (2013) Incorporating geomechanical and dynamic hydraulic-fracture-property changes into rate-transient analysis: example from the haynesville shale. *SPE Reservoir Evaluation Engineering* 16:303–316. DOI: https://doi.org/10.2118/162526-PA.

Dabiri R., Adli F., Javanbakht M. (2017) Environmental impacts of aghdarband coal mine: pollution by heavy metals. *Geopersia* 7 (2): 311–321. DOI: https://doi.org/10.22059/geope.2017.229525.648308.

Dehghan A. N., Yazdi A. (2023) A geomechanical investigation for optimizing the ultimate slope design of shadan open pit mine, iran. *Indian Geotechnical Journal* 53 (4): 859–873. DOI: https://doi.org/10.1007/s40098-022-00709-w.

El-Amin F. Mohamed (2022) Chapter three - spatial-fractional derivatives for fluid flow and transport phenomena. *Fractional Order Modeling of Dynamic Systems with Applications in Optimization, Signal Processing and Control* 2:69–96. DOI: https://doi.org/10.1016/B978-0-32-390089-8.00008-8.

Fan J., Liu P., Li J., Jiang D. (2020) A coupled methane/air flow model for coal gas drainage: model development and finite difference solution. *Process Safety and Environmental Protection* 141:288–304. DOI: https://doi.org/10.1016/j.psep.2020.05.015.

Kumar H., Mishra M. K., Mishra S. (2017) 3d modelling of coal deformation under fluid pressure using comsol multiphysics. *Journal of Engineering Science and Technology Review* 10:62–69. DOI: https://doi.org/10.25103/jestr.106.09.

Li P., Liu Q. (2022) A dual porous and fractures medium cbm numerical model development and analysis. *Journal of Petroleum Science and Engineering* 214:110511. DOI: https://doi.org/10.1016/j.petrol.2022.110511.

Ma T., Rutqvist J., Oldenburg C. M., Liu W., Chen J. (2017) Fully coupled two-phase flow and poromechanics modeling of coalbed methane recovery. *Impact of Geomechanics on Production Rate* 45:474–486. DOI: https://doi.org/10.1016/j.jngse.2017.05.024.

Mohanty M. M., Pal B. K. (2016) Simulation of fluid flow behavior during CO_2 sequestration using comsol multiphysics in coal bed. *International Journal for Scientific Research and Development* 3:12.

Ramanandraibe H. M., Ribeiro A. S., Johnson R. J., You Z. (2021) Improved modelling of pressure-dependent permeability behavior in coal based on a new workflow of petrophysics. *hydraulic fracturing and reservoir simulation* 61:106–117. DOI: https://doi.org/10.1071/aj20157.

Sirivithayapakorn S., Keller A. A. (2003) Transport of colloids in saturated porous media: a pore-scale observation of the size exclusion effect and colloid acceleration. *Water Resources Research* 39 (1-12): 859–873. DOI: https://doi.org/10.1029/2002WR001583.

Wang C., Zang Y., Wang L., Chen Z., Cui G., Fan K., Liu W. (2019) Interaction of cleat-matrix on coal permeability from experimental observations and numerical analysis. *Geofluid* 2019:1–15. DOI: https://doi.org/10.1155/2019/7474587.

Wei Z., Zhang D. (2013) A fully coupled multiphase multicomponent flow and geomechanics model for enhanced coalbed-methane recovery and CO_2 storage. *SPE Journal* 18:448–467. DOI: https://doi.org/10.12108/yxyqc.20190217.

——— (2010) Coupled fluid-flow and geomechanics for triple-porosity/dual-permeability modeling of coalbed methane recovery. *International Journal of Rock Mechanics and Mining Sciences* 47:1242–1253. DOI: https://doi.org/10.1016/j.ijrmms.2010.08.020.

Xu C., Qin L., Wang K., Sun H., Cao M. (2021) Gas seepage laws based on dual porosity and dual permeability: numerical simulation and coalbed methane extraction practice. *Energy Science and Engineering* 9:509–519. DOI: https://doi.org/10.1002/ese3.871.

Yan X., Zhang S., Tang S., Li Z., Guan W., Zhang Q., Wang J. (2021) A prediction model for pressure propagation and production boundary during coalbed methane development. *Energy Fuel* 35:1219–1233. DOI: https://doi.org/10.1021/ACS.ENERGYFUELS.0C03354.

Ye Z., Hou E., Duan Z. (2020) Micrometer-scale pores and fractures in coals and the effects of tectonic deformation on permeability based on fractal theory. *AIP Advances* 10:201–221. DOI: https://doi.org/10.1063/1.5130628.

Zhang B., Li Y., Fantuzzi N., Zhao Y., Liu Y., Peng B., Chen J. (2019) Investigation of the flow properties of cbm based on stochastic fracture network modeling. *Materials* 12:100–112. DOI: https://doi.org/10.3390/ma12152387.